Sérgio CRUZ[1,2], Flávio GASPAR[2]

University of Coimbra (1), Instituto de Telecomunicações (2)

A new method to diagnose rotor faults in 3-phase induction motors coupled to time-varying loads

Abstract. *This paper proposes a new method, based on the analysis of the active and reactive powers of the induction motor, for the diagnosis of rotor faults in motors coupled to time-varying loads. This new method is able to discriminate the presence of a true rotor fault from a time-varying load and can be used even when both the fault and the load torque variation coexist. A theoretical analysis complemented with experimental results support the effectiveness of this new diagnostic approach for the detection of rotor faults in operating three-phase induction motors.*

Streszczenie. *Zaproponowano nową metodę diagnozowania uszkodzeń wirnika bazującą na analizie mocy czynnej i biernej przy zmieniającym się obciążeniu. Wyniki eksperymentu poparte analizą teoretyczną potwierdziły skuteczność tej metody. (**Nowa metoda diagnostyki uszkodzeń wirnika indukcyjnego silnika trójfazowego dołączonego do zmiennego obciążenia**)*

Keywords: Active-reactive power, induction machines, rotor faults, load torque oscillations.
Słowa kluczowe: moc bierna i czynna, silnik indukcyjny, uszkodzenia wirnika.

Introduction

The condition monitoring of electric machines and drives is a subjected that has motivated numerous research work in the last decades. Among the different types of faults to be diagnosed, rotor cage faults in operating three-phase induction motors, whether directly connected to the mains or fed from inverters, has received considerable attention [1]-[7].

The motor current signature analysis (MCSA) is one of the most popular methods for the diagnosis of rotor faults. This type of fault can be detected by the identification in the motor current spectrum of additional components, with special emphasis on the ones at frequencies of $(1\pm 2s)f_e$, where s and f_e stand for the rotor slip and fundamental supply frequency, respectively [8]-[10]. Nevertheless, in several industrial applications, for instance in the cement industry, the motor is subjected to load torque variations of low frequency, due to cyclic variations of the industrial process. If the load torque variation has a low frequency, similar to $2sf_e$, the same spectral components mentioned above can be found in the motor current spectrum even when the motor is in healthy conditions. This limitation is shared by many other diagnostic approaches of rotor faults.

Some work has been done in the past, in an attempt to discriminate the occurrence of a rotor fault from other phenomena, no matter the type of load coupled to the motor. In [11, 12] that is accomplished by comparing the actual stator current with the one obtained from a machine model which includes the load effects. The difference between these two signals provides a quantity which, in theory, is independent of load variations. The major drawback of this scheme is its heavy dependence on the accurate estimation of the motor parameters, which includes the stator and rotor resistances and all motor inductances.

In [1, 2, 13] was proposed to use the current Park's Vector in a synchronous reference frame to discriminate rotor faults from load torque variations. The results shown demonstrate that the current loci obtained in these two cases is different, providing a means to separate the two phenomena. Unfortunately, if they are present at the same time, no simple representation is obtained, leading to a diagnosis which may not be conclusive.

A time-frequency approach was proposed in [14] in order to detect rotor faults even when the machine is subjected to a torque dip. The results show that it is possible to discriminate the presence of three broken rotor bars and a torque dip but the obtained current spectrograms are difficult to interpret by a non-expert and it is not clear if an incipient rotor fault can be detected using this diagnostic methodology.

Other methods proposed for the same purpose include the use of neural networks [15]. In these cases, the disadvantage is the necessity of training the neural network, which may not be feasible in a machine already running in an industrial environment.

More recently, the *p-q* theory was also used to calculate the instantaneous active and reactive currents, thus allowing to discriminate a rotor fault from a time-varying load [16]. Although the obtained results are promising, there still exists some kind of ambiguity in the discrimination of the two phenomena, especially if the load variation is unknown.

Given the state-of-the-art in this field, this paper proposes a new methodology for the diagnosis of rotor faults, independently of the type of load coupled to the motor. The method relies on a combined analysis of the active and reactive powers of the motor and is able to detect a rotor fault and distinguish it from a load torque variation even when they occur simultaneously.

Analysis of rotor faults and time-varying loads

A. Previous work

In an induction motor with a rotor fault, the supply currents contain spectral components at frequencies of $(1\pm 2s)f_e$. The same happens if instead of a rotor fault, the motor is coupled to a mechanical load that imposes a periodic load torque oscillation with a frequency of $2sf_e$. Hence, the simple analysis of the amplitude spectrum of the motor supply currents does not allow to discriminate these two phenomena. However, if these currents are transformed to *dq* axes and analysed in a synchronous reference frame (rotating at the angular supply frequency), more information can be extracted from those signals as the faulty components introduced by the rotor fault will appear in that reference frame at a frequency of $(1\pm 2s)f_e - f_e = \pm 2sf_e$. That was already seen in [1, 2], where this reference frame was used to analyse the locus of the current space vector when the induction motor had rotor faults or was coupled to time-varying loads. In the first case, the current locus obtained is an ellipse whose origin is the current vector given by the sum of two current vectors (each one corresponding to one of the two faulty current components at frequencies of $(1\pm 2s)f_e$), rotating in opposite directions, at an angular frequency of $2\pi\times 2sf_e$.

When the inertia of the load is very high, the speed oscillations of the motor will be very small, and that ellipse will tend to a circumference. On the other hand, for extremely low values of the inertia, the ellipse tends to degenerate into a straight line oriented along the second quadrant of the axes.

When the motor, in healthy conditions, is coupled to a time-varying load, the current locus obtained is almost a straight line, in this case oriented along the first quadrant of the axes, for torque oscillations of low amplitude and low frequency. When the frequency of the torque oscillation increases, the pattern obtained resembles an ellipse whose major axis is progressively oriented along the *q*-axis.

The orientation of the major axis of these ellipses is related to the difference of phase between the *d* and *q* current components in the synchronous reference, thus leading to the necessity of performing an analytic study about these quantities in that reference frame. The next section deals with the presentation of a linearized induction motor model developed with that aim.

B. Linearized induction motor model [17]

A simplified induction motor model will be used to study the effects of rotor faults and time-varying loads. The model relies on the use of an asymmetrical two-phase induction motor, whose details can be found in [18].

As demonstrated in several papers, n_F contiguous broken bars in a rotor cage with N_b bars can be represented in an approximate way by the inclusion of an additional resistance in one of the phases of an equivalent three-phase slip-ring machine [19]. If this machine is transformed into an equivalent asymmetrical two-phase machine, the additional resistance R_F that appears in one of the phases is given by [20-22]:

$$\frac{R_F}{2} \approx \frac{n_F}{N_b} R_r \tag{1}$$

where R_r stands for the rotor resistance of the two-phase machine in healthy conditions. Without loss of generality, the fault may be considered located along the *d*-axis of the rotor. In that case, the resistances of the two rotor windings will be $R_{rd}=R_r+R_F$ and $R_{rq}=R_r$.

Writing the voltage equations of this machine in *dq* axes rotating at an arbitrary angular speed ω_a, and if a rotor fault or time-varying load is considered, the rotor speed will not be constant, leading to a system of non-linear differential equations. Hence, that system of equations can only be solved by numerical methods, does not providing an analytical solution to the problem. To overcome this limitation, a model linearization is performed around an operating point. This allows to obtain analytical solutions for the motor supply current components, which will be used later on in the calculation of the active and reactive powers of the machine needed for diagnostic purposes.

In a synchronously rotating reference frame ($\omega_a=\omega_e$) with the *q*-axis aligned with the stator voltage space vector, the linearized voltage equations of the faulty machine are given by (2) and (3) [17].

$$\begin{bmatrix} 0 \\ U \\ 0 \\ 0 \end{bmatrix} = \begin{bmatrix} R_s & -\omega_e L_s & 0 & -\omega_e L_m \\ \omega_e L_s & R_s & \omega_e L_m & 0 \\ 0 & -\bar{s}\omega_e L_m & \bar{R}_r & -\bar{s}\omega_e L_r \\ \bar{s}\omega_e L_m & 0 & \bar{s}\omega_e L_r & \bar{R}_r \end{bmatrix} \begin{bmatrix} \bar{i}_{ds} \\ \bar{i}_{qs} \\ \bar{i}_{dr} \\ \bar{i}_{qr} \end{bmatrix} \tag{2}$$

In (2)-(3) R_s, $\bar{R}_r$, L_s, L_r, L_m stand for the stator resistance, average value of the rotor resistances ($R_r+R_F/2$), stator inductance, rotor inductance and mutual inductance between stator and rotor windings, respectively. The operator $p=d/dt$, $\Delta R_r = R_F/2$, $\theta_{s\omega}$ represents the slip angle, $\bar{s}$ stands for the average rotor slip and p_p is the number of pole-pairs. Δt_L is the load torque variation (equals zero if the load torque is constant). All rotor quantities and motor parameters are referred to the stator. A dash over a quantity denotes its average (steady-state) value and the prefix Δ corresponds to its incremental value. It is assumed that the motor is supplied by a balanced voltage supply system ($u_{qs}=U=\text{c.te}$).

The previous equations, complemented with the equation of torque, can be used to obtain analytical solutions for the stator current components i_{ds} and i_{qs}. These analytical solutions are, however, quite long to be presented here. Even though, whether for the case of a rotor fault or for a time-varying load, the current components are of the form

$$i_{ds}(t) = \bar{i}_{ds} + \Delta i_{ds} = \bar{i}_{ds} + A\cos\left(2\bar{s}\omega_e t + \alpha\right) \tag{4}$$

$$i_{qs}(t) = \bar{i}_{qs} + \Delta i_{qs} = \bar{i}_{qs} + B\cos\left(2\bar{s}\omega_e t + \beta\right) \tag{5}$$

where $\bar{i}_{ds}$, $\bar{i}_{qs}$ are constants that depend on the motor operating point (load level). $A=\Delta\hat{i}_{ds}$, $B=\Delta\hat{i}_{qs}$, α, β are values that depend on the motor parameters, fault extension (if a rotor fault is present), load inertia and motor operating point.

The angles α, β contain vital information that can be used to distinguish the rotor fault from the time-varying load. For a time-varying load α and β have similar values provided that: (i) the torque oscillations are of low amplitude and (ii) their frequency is relatively low (say below 10 Hz for a supply system of 50 Hz). Nevertheless, if the stator resistance of the stator windings of the motor is high (like in the case of low-voltage small-power motors), the angles α and β may differ by an angle which may not be negligible, although always less than ≈ 90 deg for the typical parameters of an induction motor.

(3)

$$\begin{bmatrix} 0 \\ 0 \\ 0 \\ 0 \\ \Delta t_L \end{bmatrix} = \Delta R_r \left[\begin{array}{cccc|c} 0 & 0 & 0 & 0 & 0 \\ 0 & 0 & 0 & 0 & 0 \\ 0 & 0 & \cos(2\theta_{s\omega}) & -\sin(2\theta_{s\omega}) & 0 \\ 0 & 0 & -\sin(2\theta_{s\omega}) & -\cos(2\theta_{s\omega}) & 0 \\ \hline 0 & 0 & 0 & 0 & 0 \end{array}\right] \begin{bmatrix} \bar{i}_{ds} \\ \bar{i}_{qs} \\ \bar{i}_{dr} \\ \bar{i}_{qr} \\ \bar{s} \end{bmatrix} + \left[\begin{array}{cccc|c} R_s + pL_s & -\omega_e L_s & pL_m & -\omega_e L_m & 0 \\ \omega_e L_s & R_s + pL_s & \omega_e L_m & pL_m & 0 \\ pL_m & -\bar{s}\omega_e L_m & \bar{R}_r + pL_r & -\bar{s}\omega_e L_r & -\omega_e\left(L_m\bar{i}_{qs} + L_r\bar{i}_{qr}\right) \\ \bar{s}\omega_e L_m & pL_m & \bar{s}\omega_e L_r & \bar{R}_r + pL_r & \omega_e\left(L_m\bar{i}_{ds} + L_r\bar{i}_{dr}\right) \\ \hline -\frac{3}{2}p_p L_m\bar{i}_{qr} & \frac{3}{2}p_p L_m\bar{i}_{dr} & \frac{3}{2}p_p L_m\bar{i}_{qs} & -\frac{3}{2}p_p L_m\bar{i}_{ds} & p\frac{J}{p_p}\omega_e \end{array}\right] \begin{bmatrix} \Delta i_{ds} \\ \Delta i_{qs} \\ \Delta i_{dr} \\ \Delta i_{qr} \\ \Delta s \end{bmatrix}$$

On the other hand, for the case of a rotor fault, the current space vector locus is an ellipse with the major axis oriented along the second quadrant of the *dq* axes. The mathematical expressions that describe the *dq* current components are similar to (4)-(5) with the exception of the values assumed by the angles α, β and the new current amplitudes $\Delta\hat{i}_{ds}$ and $\Delta\hat{i}_{qs}$. In general, for rotor faults $\Delta\hat{i}_{ds} > \Delta\hat{i}_{qs}$ while for time-varying loads $\Delta\hat{i}_{ds} << \Delta\hat{i}_{qs}$.

By varying the combined inertia of the rotor-mechanical load, the orientation and ellipticity of the figure obtained changes. As $J \to \infty$ the current locus tends to a circumference (no speed oscillations meaning that the amplitude of spectral component of the motor supply currents at the frequency $(1+2s)f_e$ tends to zero). In addition, when $J \to \infty$, $\Delta\hat{i}_{ds} \approx \Delta\hat{i}_{qs}$ and $\alpha \approx \beta - 90$. Hence, the conclusion is that the angles α and β contain vital information which allows to discriminate a rotor fault from a time-varying load.

Let us define the angle $\gamma = \alpha - \beta$, properly reduced to the range $[-180^\circ,\ 180^\circ]$. Based on the analysis carried out before, if $|\gamma| \in [0,\ \approx 90^\circ]$ the motor is coupled to a time-varying load. Conversely, if $|\gamma| \in]\approx 90^\circ,\ 180^\circ]$ the motor has a rotor fault. No ambiguity exists in the region where $|\gamma| \approx 90^\circ$. In fact, in that region, a time-varying load leads to values of $\Delta\hat{i}_{ds} < \Delta\hat{i}_{qs}$ while for broken rotor bars $\Delta\hat{i}_{ds} \approx \Delta\hat{i}_{qs}$. Hence, the combined analysis of these fault indicators allows to reliably detect and discriminate these two motor operating conditions no matter the operating point of the motor.

It should also be pointed out that there is no need to know the exact value of γ to perform the diagnosis but solely to see in which interval its modulus falls into. This is an advantage especially because the exact value of this angle depends on numerous motor parameters, extension of the fault, load level and moment of inertia.

The method to diagnose and discriminate rotor faults from time-varying loads

Considering that the motor supply voltage components in the synchronous reference frame are given by $u_{ds}(t) = 0$, $u_{qs}(t) = U$, the motor instantaneous active power (*p*) and reactive power (*q*) can be calculated using

$$p(t) = \frac{3}{2}\left(u_{ds}^a i_{ds}^a + u_{qs}^a i_{qs}^a\right) = \frac{3}{2}u_{qs} i_{qs} = \frac{3}{2}U i_{qs}(t) \tag{6}$$

$$q(t) = \frac{3}{2}\left(u_{qs}^a i_{ds}^a - u_{ds}^a i_{qs}^a\right) = \frac{3}{2}u_{qs} i_{ds} = \frac{3}{2}U i_{ds}(t)\,. \tag{7}$$

where superscript a denotes an arbitrary reference frame.

Substituting (4)-(5) into (6)-(7) one obtains

$$p(t) = \overline{p} + \Delta p(t) = \frac{3}{2}U\,\overline{i}_{qs} + \frac{3}{2}U\Delta\hat{i}_{qs}\cos\left(2\overline{s}\,\omega_e t + \beta\right) \tag{8}$$

$$q(t) = \overline{q} + \Delta q(t) = \frac{3}{2}U\,\overline{i}_{ds} + \frac{3}{2}U\Delta\hat{i}_{ds}\cos\left(2\overline{s}\,\omega_e t + \alpha\right)\,. \tag{9}$$

Equations (8)-(9) show that the angles α, β can be easily measured by performing a spectrum analysis to the total reactive and active powers of the motor, respectively. One advantage of using the power signals instead of the current signals directly is that the equations used for the calculation of the two powers are valid in any reference frame, hence their calculation can be advantageously performed in the stationary reference frame, thus avoiding the necessity of performing a reference frame transformation.

The diagnosis procedure should then consist in the analysis of the amplitude spectra of p and q in the low frequency range (wide enough to contain the frequency $2\overline{s}f_e$) to search for spectral components which may exist in this frequency region (if a symmetrical motor is considered, coupled to a constant load, no spectral components should be found in this frequency range as the quantities under analysis represent total active and reactive powers of the motor). If spectral components are found in any of the amplitude power spectra, the exact value of their frequency should be recorded and the phase spectra of the these two power signals analysed at the same frequencies in order to calculate the angle $|\gamma|$. The range in which $|\gamma|$ falls into will determine the origin of the spectral component(s) (intrinsic rotor fault or mechanical load variation).

A problem with the power signals in medium/high power motors is that the average slip of these motors is very small, meaning that the spectral components introduced by a potential rotor fault will be close to the dominant dc component of the active and reactive powers. This neighbourhood can obscure the presence of those characteristic components. To overcome this problem, the dc component of the two power signals should be removed prior performing the spectrum analysis.

The diagnostic process can thus be summarized as follows:

a) Calculation of the active and reactive powers of the motor using the voltage and current signals in a stationary reference frame

b) Removal of the dc components of p and q

c) Perform a FFT to the obtained signals and search for spectral components in both spectra in the low frequency range (0-10 Hz, as an indicative range)

d) At the frequencies found in the previous step, check the difference of phase between p and q and refer the absolute value of the resulting angle ($|\gamma|$) to the range $[0,\ 180^\circ]$: if this angle is lower than 90 deg, that indicates the presence of a time-varying load; if it is higher than 90 deg, a rotor fault was found; if $|\gamma| \approx 90^\circ$ check the amplitudes of Δp and Δq measured in c): if $\Delta q < \Delta p$ it is a time-varying load, otherwise a rotor fault was found.

Experimental results

To validate the proposed diagnostic approach several experimental tests were carried out.

The experimental setup is based on a WEG® W21, 3 kW, 400 V, 50 Hz, 4-pole, 3-phase induction motor connected to a 400 V balanced voltage supply system. This test motor is mechanically coupled to another induction motor, direct torque controlled. A dSPACE 1103 development board ensures the implementation of the control strategy of the second motor and allows the user to impose any desired load torque profile, whether constant or variable in time.

Two additional rotors were used in the test motor, identical to the original one, in which 1 and 2 broken bars were emulated by drilling a hole in each bar near to an end-ring.

Fig. 1 shows the experimental results obtained when the induction motor is running at 75% rated load (constant torque), with one broken rotor bar. From top to bottom, the figures show the amplitude and phase spectra of the

oscillating (ac) components of the active and reactive powers of the motor and the modulus of angle γ. In this test $|\gamma|$=178.2 deg that, as expected, is higher than the 90 deg above which a rotor fault is identified. These results also show that the rotor fault creates an oscillation in the reactive power with an amplitude higher than the one created in the active power, which is in good agreement with what was predicted by theory. It is interesting to note that besides the spectral components at a frequency of $2\bar{s}f_e$, the two power spectra also contain a component at a frequency of $4\bar{s}f_e$, whose origin are second-order effects of a rotor fault (corresponding to current components at frequencies of $(1\pm 4\bar{s})f_e$). Even for the second order effects, the value of $|\gamma|$ is clearly higher than 90 deg, hence showing that the origin of these components is the rotor fault

Fig. 2 shows the results obtained when the induction motor runs in healthy conditions, coupled to a time-varying load with a sinusoidal oscillating component at a frequency of 2.5 Hz, superimposed to a constant term. In this test $|\gamma|$=34.98 deg, indicating that the spectral components found in the active and reactive powers at 2.5 Hz are introduced by the mechanical load and not due to a rotor asymmetry. In addition, the oscillations found in the active power are higher than the ones of the reactive power, once again supporting the theory behind the diagnostic method. It should be noted that in this case, the motor current signature analysis would be totally ineffective as a diagnostic tool because the current spectrum contains two sideband components at frequencies of 47.5 Hz and 52.5 Hz, whose origin could mean a rotor fault or a time-varying load. These results also demonstrate the high sensitivity of this diagnostic method, as besides the load torque oscillations, the method also detected the presence of a residual rotor asymmetry. This was confirmed with an additional test, during which the motor was run at a constant load and with a rotor in healthy conditions.

Fig. 3 shows the results with the motor running with a rotor fault and coupled to a time-varying load with a sinusoidal oscillating component at a frequency of 5 Hz.

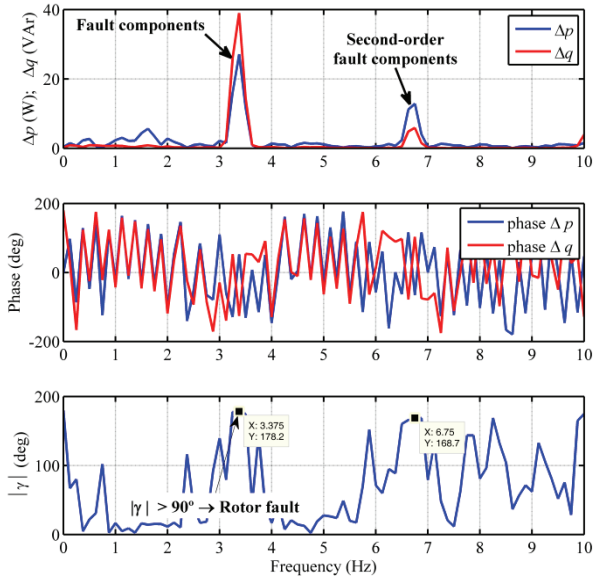

Fig. 1. Experimental results showing the diagnosis of a rotor fault (1 broken bar) in a motor running with a constant load torque.

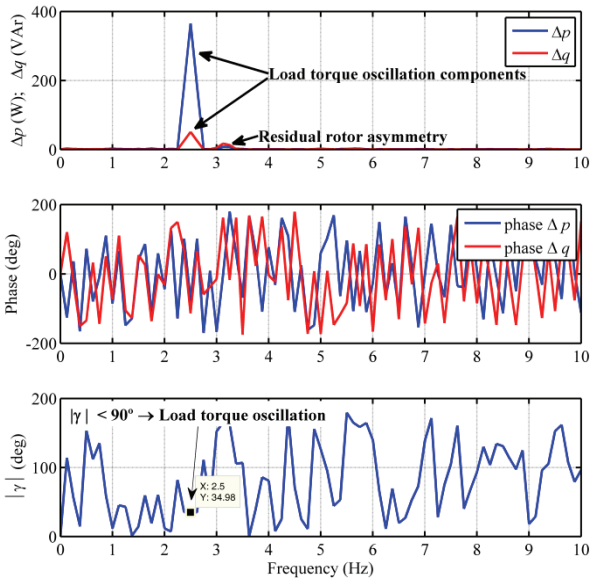

Fig. 2. Motor running in healthy conditions, coupled to an oscillating load torque with a frequency of 2.5 Hz.

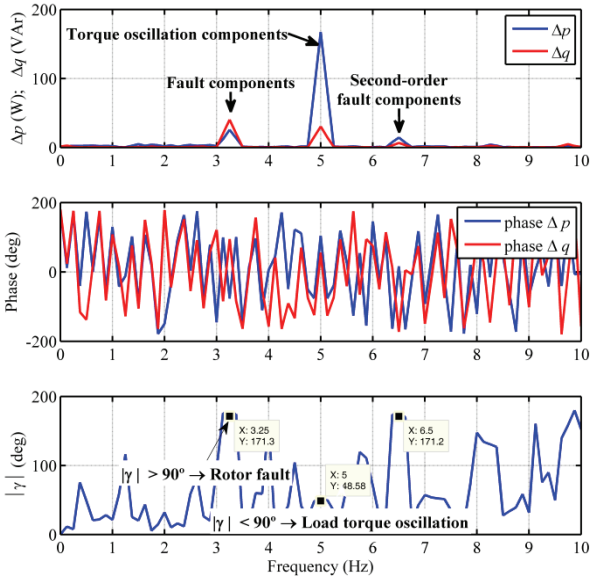

Fig. 3. Motor running with 1 broken rotor bar and coupled to an oscillating load torque with a sinusoidal component at a frequency of 5 Hz.

The obtained results show two dominant spectral components in the amplitude spectra of the active and reactive powers, at frequencies of 3.25 Hz and 5 Hz. At these frequencies, $|\gamma|$ was 171.3 deg and 48.58 deg, respectively, the first value indicating the presence of a rotor fault and the second one related to the time-varying load.

These results clearly demonstrate that when rotor faults and time-varying loads coexist, the proposed diagnostic method is capable of discriminating the two phenomena even when the frequencies at which they manifest themselves are very close, as in this example.

To end this section, some additional results are shown in Fig. 4, where the motor was run with the rotor in healthy conditions but coupled to a load which imposes a square wave load torque oscillation. This type of load was used for two main reasons: (i) to somehow emulate motors coupled to impact loads (compressors, for instance) and (ii) to

create a torque variation with several spectral components in the low frequency range.

Once again, the diagnostic method is able to demonstrate that the origin of all detected spectral components is the load torque variation and not an eventual rotor fault.

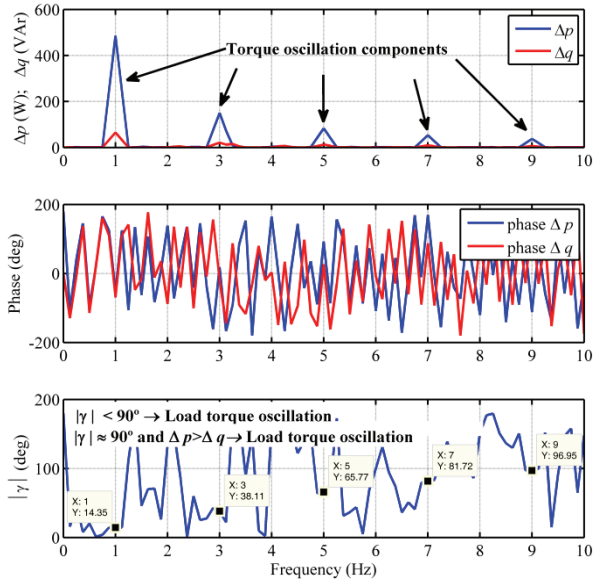

Fig. 4. Motor running in healthy conditions, coupled to an oscillating load torque, of square wave type, with a fundamental frequency of 1 Hz.

Conclusion

This paper presented a new diagnostic method, based on the analysis of active and reactive powers of an induction machine, to detect and discriminate rotor faults from time-varying loads. The combined analysis of the amplitude and phase spectra of the active and reactive powers of the motor can be used with great success in the discrimination of these two phenomena, without the need of any motor parameters, making this method particularly attractive to be used in an industrial environment. It is noteworthy the sensitivity and discriminating power demonstrated by this method, by detecting residual rotor asymmetries and clearly distinguish them from load torque variations of different kinds.

The implementation of this diagnostic approach only requires the measurement of two motor supply currents and two line to line voltages. Hence, it may constitute a valuable aid for the maintenance personnel responsible for motors coupled to any type of mechanical load, whether constant or variable in time.

The authors wish to acknowledge the financial support of the Portuguese Foundation for Science and Technology, under Project Number PTDC/EEA-ENE/67350/2006.

REFERENCES

[1] Cruz S. M. A. and Cardoso A. J. M., Rotor cage fault diagnosis in operating three-phase induction motors, under the presence of time-varying loads, Proc. EPE, (2001).

[2] Cruz S. M. A. and Cardoso A. J. M., Discriminating between rotor asymmetries and time-varying loads in three-phase induction motors, Proc. COMADEM, (2001), 319-327.

[3] Zhenxing L., Xianggen Y., Zhe Z., Deshu Chen A., and Wei Chen A., Online rotor mixed fault diagnosis way based on spectrum analysis of instantaneous power in squirrel cage induction motors, *IEEE Trans. Energy Conv.*, 19 (2004), 485-490.

[4] Drif M. and Cardoso A. J. M., The Use of the Instantaneous-Reactive-Power Signature Analysis for Rotor-Cage-Fault Diagnostics in Three-Phase Induction Motors, *IEEE Trans. Industrial Electronics*, 56 (2009), 4606-4614.

[5] Muller G. H. and Landy C. F., A novel method to detect broken rotor bars in squirrel cage induction motors when interbar currents are present, *IEEE Trans. Energy Conv.,* 18 (2003), 71-79.

[6] Mirafzal B. and Demerdash N. A. O., On innovative methods of induction motor interturn and broken-bar fault diagnostics, *IEEE Trans. Industry Appl*., 42 (2006), 405-414.

[7] Thomas V., Vasudevan K., and Kumar V. J., Online cage rotor fault detection using air-gap torque spectra, *IEEE Trans. Energy Conv.,* 18 (2003), 265-270.

[8] Nandi S., Toliyat H. A., and Xiaodong L., Condition monitoring and fault diagnosis of electrical motors-a review, *IEEE Trans. Energy Conv.,* 20 (2005), 719-729.

[9] Henao H., Razik H., and Capolino G., Analytical approach of the stator current frequency harmonics computation for detection of induction machine rotor faults, *IEEE Transactions on Industry Appl.,* 41 (2005), 801-807.

[10] Jee-Hoon J., Jong-Jae L., and Bong-Hwan K., Online Diagnosis of Induction Motors Using MCSA," *IEEE Trans. Industrial Electronics*, 53 (2006), 1842-1852.

[11] Schoen R. R. and Habetler T. G., Effects of time-varying loads on rotor fault detection in induction machines, *IEEE Trans. Industry Appl.,* 31 (1995), 900-906.

[12] Schoen R. R. and Habetler T. G., Evaluation and implementation of a system to eliminate arbitrary load effects in current-based monitoring of induction machines, *IEEE Trans. Industry Appl.*, 33 (1997), 1571-1577.

[13] Cruz S. M. A. and Cardoso A. J. M., Further developments on the use of the synchronous reference frame current Park's Vector Approach, Proc. IEEE SDEMPED, (2001), 467-472.

[14] Bacha K., Gossa M., Henao H., and Capolino G. A., A time-frequency method for multiple fault detection in three-phase induction machines, Proc. IEEE SDEMPED, (2005).

[15] Salles G., Filippetti F., Tassoni C., Crellet G., and Franceschini G., Monitoring of induction motor load by neural network techniques, *IEEE Trans. Power Electronics*, 15 (2000), 762-768.

[16] Bossio G. R., Angelo C. H., Bossio J. M., Pezzani C. M., and Garcia G. O., Separating Broken Rotor Bars and Load Oscillations on IM Fault Diagnosis Through the Instantaneous Active and Reactive Currents, *IEEE Trans. Industrial Electronics*, 56 (2009), 4571-4580.

[17] Cruz S. M. A. and Gaspar F., A new PQ method to diagnose rotor faults in three-phase induction motors coupled to time-varying loads, Proc. IEEE SDEMPED, (2011).

[18] Cruz S. M. A., Stefani A., Filippetti F., and Cardoso A. J. M., A New Model-Based Technique for the Diagnosis of Rotor Faults in RFOC Induction Motor Drives, *IEEE Trans. Industrial Electronics*, 55 (2008), 4218-4228.

[19] Filippetti F., Martelli M., Franceschini G., and Tassoni C., Development of expert system knowledge base to on-line diagnosis of rotor electrical faults of induction motors, Proc. IEEE IAS Annu. Meeting, 1 (1992), 92-99.

[20] Bellini A., Filippetti F., Franceschini G., and Tassoni C., Closed-loop control impact on the diagnosis of induction motors faults, *IEEE Transactions on Industry Appl.*, 36 (2000), 1318-1329.

[21] Bellini A., Franceschini G., Tassoni C., and Toscani A., Assessment of induction machines rotor fault severity by different approaches, Proc. IEEE IECON, (2005), 1461-1466.

[22] Bellini *et al.*, Thorough Understanding and Experimental Validation of Current Sideband Components in Induction Machines Rotor Monitoring, Proc. IEEE IECON, (2006), 4957-4962.

***Authors**: Prof. Dr. Sérgio Cruz, Department of Electrical and Computer Engineering, Pólo II – Pinhal de Marrocos, 3030-290 Coimbra, Portugal, E-mail: smacruz@deec.uc.pt; Mr. Flávio Gaspar, Instituto de Telecomunicações, edifício DEEC, Pólo II – Pinhal de Marrocos, 3030-290 Coimbra, Portugal, E-mail: faagaspar@gmail.com.*